Nucleic Acids Research, 1999, Vol. 27, No. 10 **2189–2195**

Structural properties of DNA:RNA duplexes containing 2′-O-methyl and 2′-S-methyl substitutions: a molecular dynamics investigation

Divi Venkateswarlu, Kenneth E. Lind, V. Mohan[1], Muthiah Manoharan[1] and David M. Ferguson*

Department of Medicinal Chemistry and Minnesota Supercomputer Institute, University of Minnesota, Minneapolis, MN 55455, USA and [1]ISIS Pharmaceuticals, 2922 Faraday Avenue, Carlsbad, CA 92008, USA

Received January 7, 1999; Revised and Accepted March 30, 1999

ABSTRACT

The physical properties of a DNA:RNA hybrid sequence d(CCAACGTTGG)•(CCAACGUUGG) with modifications at the C2′-positions of the DNA strand by 2′-O-methyl (OMe) and 2′-S-methyl (SMe) groups are studied using computational techniques. Molecular dynamics simulations of SMe_DNA:RNA, OMe_DNA:RNA and standard DNA:RNA hybrids in explicit water indicate that the nature of the C2′-substituent has a significant influence on the macromolecular conformation. While the RNA strand in all duplexes maintains a strong preference for C3′-endo sugar puckering, the DNA strand shows considerable variation in this parameter depending on the nature of the C2′-substituent. In general, the preference for C3′-endo puckering follows the following trend: OMe_DNA>DNA>SMe_DNA. These results are further corroborated using *ab initio* methods. Both gas phase and implicit solvation calculations show the C2′-OMe group stabilizes the C3′-endo conformation while the less electronegative SMe group stabilizes the C2′-endo conformation when compared to the standard nucleoside. The macromolecular conformation of these nucleic acids also follows an analogous trend with the degree of A-form character decreasing as OMe_DNA:RNA>DNA:RNA>SMe_DNA:RNA. A structural analysis of these complexes is performed and compared with experimental melting point temperatures to explain the structural basis to improved binding affinity across this series. Finally, a possible correlation between RNase H activity and conformational changes within the minor groove of these complexes is hypothesized.

INTRODUCTION

The development of therapeutically useful antisense oligonucleotide compounds has met with varied success over the last decade (1,2). Although a wide variety of chemical modifications has been proposed to modulate antisense activity, many fail to impart the desired balance in selectivity, nuclease activity and binding affinity to target mRNAs (3–5). One of the more successful modifications involves the substitution of the standard phosphate backbone with a phosphorothioate moiety (6–8). While these compounds show nuclease resistance as well as RNase H activity when complexed with RNA, their binding affinity is not optimal. This is due, in part, to the stereochemistry created at the phosphate center, which can either adopt the R or S configuration, leading to diastereomeric mixtures. It is now well known that the diastereomers have different physical properties which may have a direct impact on non-selective binding *in vivo* and reduced binding affinities to the target mRNA (9,10). Another class of modifications, which could be deemed second generation antisense oligonucleotides, involves the modification of the C2′-OH of the standard ribose sugar. These derivatives were developed based on the premise that electronegative substituents in the C2′-position would favor C3′-endo sugar puckering (11). This, in turn, would preorganize the antisense oligonucleotide strand to adopt an A-form type geometry, leading to higher binding affinities (3,12,13).

While many of the C2′-modified oligonucleotides show higher affinity for target RNAs as compared to phosphorothioates and standard nucleic acid strands, most fail to recruit RNase H degradation of the complementary mRNA *in vitro* (14–16). Although no direct structural evidence has been gathered to explain this failure to activate RNase H, it is commonly thought that the conformation of the hybrid duplex plays a dominant role in enzyme activation. RNase H selectively degrades the RNA strand of wild-type RNA:DNA complexes *in vivo*. It is thought to attack the complex through specific interactions with the minor groove of the nucleic acids (17). RNA:DNA complexes have an intermediate minor groove width between that known for DNA:DNA and RNA:RNA duplexes (18). It is therefore postulated that C2′-modifications produce AO:RNA complexes that may be too similar to native RNA:RNA (i.e. A-form geometries) or too dissimilar to native DNA:RNA conformations (19). A second, less frequently cited concern arises from the position of the C2′-substituent. Modifications at this position tend to point into the minor groove in the A-form geometry, potentially disrupting the enzymes interaction with the minor groove.

Not all C2′-substitutions follow the general rule of favoring C3′-endo puckering. Less electronegative groups, such as S-methyl or alkyl sidechains, tend to enhance C2′-endo puckering in ribose sugars (20–23). This, in turn, is thought to lead to

*To whom correspondence should be addressed. Tel: +1 612 626 2601; Fax: +1 612 626 4429; Email: ferguson@vwl.medc.umn.edu

destabilization of the AO:RNA complex. In fact, the S-methyl substitution is known to destabilize AO:RNA complexes by ~1.5° per base pair when compared with native DNA:RNA hybrids (unpublished results, ISIS Pharmaceuticals). What is not known, however, is whether these substitutions induce AO:RNA duplex conformations that are suitable candidates for RNase H.

In this study, we examine the structural properties of antisense oligonucleotides that are modified at the C2′ position by O-methyl and S-methyl groups using a combination of molecular dynamics, molecular mechanics and *ab initio* calculations. In particular, we are interested in understanding the conformational effects induced by the C2′ substitution in both the free nucleoside and AO:RNA complex. Based on template structures derived from native RNA:DNA and ideal A/B form geometries, molecular dynamics simulations are performed in explicit water in an effort to rationalize the observed differences in experimental melting temperatures for these two modifications. Structural analyses are also presented and compared with native RNA:DNA hybrid structures to investigate changes in the sugar puckering, base stacking and minor groove dimensions, especially as they relate to binding affinity and potential RNase H activity.

MATERIALS AND METHODS

The initial coordinates of the hybrid d(CCAACGTTGG)•r(CCAACGUUGG) were taken from the average DNA:RNA structure reported by Kollman and Cheatham in a prior computational study of nucleic acid conformation (24). This sequence has been shown to produce equilibrium structures in good agreement with experimental observations. This structure was further modified to include 2′-S-methyl groups to complete the setup of the SMe_DNA:RNA complex. The starting coordinates for the OMe_DNA:RNA structure were generated in the standard A-form (Arnott's) geometry using the NUCGEN module of the AMBER4.1 package (25) with appropriate C2′-O-methyl substitutions. To each complex, a total of 18 neutralizing counter-ions were added at the bifurcating positions of O-P-O angle at a distance of 4.5 Å from the phosphorus atom. The hybrid duplexes with counter-ions were then immersed in a periodic box of TIP3P water (26). This produced corresponding systems sizes of 3359/61.40 Å × 46.29 Å × 43.69 Å, 2586/60.23 Å × 41.55 Å × 40.04 Å and 3278/58.48 Å × 43.86 Å × 41.63 Å (no. of waters/box dimensions) for the DNA:RNA, OMe_DNA:RNA and SMe_DNA:RNA, respectively.

All molecular dynamics simulations reported in this work were performed using the SANDER module of AMBER4.1. Long range interactions were treating using the particle mesh Ewald (PME) method (27). The PME charge grid spacing was ~1.0 Å, and the charge grid was interpolated using a cubic B-spline of the order of four with the direct sum tolerance of 0.00001 at the 9 Å direct space cutoff. A constant temperature and pressure (300 K/1 atm) was maintained throughout the simulations using the Berendsen scaling algorithm with coupling constants of 0.2 ps in both cases. A time step of 0.002 ps was used to integrate the equations of motion with a non-bonded pairlist update frequency of 0.020 ps. All bonds involving hydrogen were constrained using the SHAKE algorithm (28). Before beginning the 'production-run' simulations, the following equilibration protocol was followed. First, the water molecules and counter-ions in the periodic box were energy minimized to a r.m.s. gradient of 0.1, followed by 10 ps of molecular dynamics at 300 K. Second, the whole system, including solute, counter-ions and waters, was subjected to 1000 steps of energy minimization to remove close contacts and relax the system. Lastly, external positional restraints were added to the solute atoms and gradually reduced over 60 ps of MD at 300 K. This was accomplished using three 20 ps intervals of MD with positional force constants of 10, 1 and 0.1 kcal/molÅ^2 to slowly bring the system to equlibration at 300 K. All simulations were continued for 1 ns and the coordinates were written every 2 ps and stored for subsequent analysis. The resulting trajectories were analyzed using the CARNAL module of AMBER4.1. The average structures of the three hybrids DNA:RNA, OMe_DNA:RNA and SMe_DNA:RNA were obtained by averaging over the last 500 ps of dynamics. The standard helicoidal parameters of the averaged DNA structures were deduced using CURVES5.1 program (29). All calculations were performed on a Silicon Graphics ORIGIN2000 fitted with 32 SGI/R10000 processors using the MPI version of the SANDER program. Each simulation demanded ~950 s of CPU time per ps of simulation time on one processor.

Parameters

The force-field parameters for the 2′-OCH3 and -SCH3 groups were adapted from the standard PARM94 database of the AMBER4.1 package. The general procedures outlined by Cornell *et al*. were followed here in parameterization (30). The required charges for both groups were derived using the RESP approach outlined by Bayly *et al*. (31) Two model compounds were used: $(CH3)_2$-CH-O-CH_3 and $(CH3)_2$-CH-S-CH_3. The charges on the --OCH3 and --SCH3 groups (+0.1953 on each group) were set to balance that of the 2′-hydroxyl group (–0.1953) of the standard ribose sugar, thereby maintaining the overall charge balance in the ribofuranosyl system consistent with the AMBER/PARM94 database. The required ESP grid for the generation of RESP-fit charges and HF/SCF-MO calculations on model nucleosides were calculated using the HF/6–31G* basis set with Gaussian94 suite of programs (32). A listing of the charges and the atom types used for -OMe and -SMe groups are given in the Supplementary Material.

RESULTS AND DISCUSSION

Ribose conformations in C2′-modified nucleosides

In order to understand the influence of 2′-O-methyl and 2′-S-methyl groups on the conformation of nucleosides, we have evaluated the relative energies of the 2′-O- and 2′-S-methylguanosine, along with normal deoxyguanosine and riboguanosine, starting from both C2′-endo and C3′-endo conformations using *ab initio* HF/SCF-MO theory. All the structures were fully optimized at HF/6–31G* level and single point energies with electron-correlation were obtained at the MP2/6–31G*//HF/6–31G* level. As shown in Table 1, the C2′-endo conformation of deoxyguanosine is estimated to be 0.6 kcal/mol more stable than C3′-endo conformation in the gas-phase. The conformational preference of the C2′-endo over the C3′-endo conformation appears to be less dependent on electron correlation as revealed by the MP2/6–31G*//HF/6–31G* values which also predict the same difference in energy. The opposite trend is noted for riboguanosine. At the HF/6–31G* and MP2/6–31G*//HF/6–31G* levels, the C3′-endo form of riboguanosine is shown to be ~0.65 and 1.41 kcal/mol more stable than C2′-endo form, respectively.

Table 1. Relative energies of the C3′-endo and C2′-endo conformations of representative nucleosides

	HF/6–31G*	MP2/6–31G**[a]	SCI-PCM[a]	AMBER94
dG	0.60	0.56	0.88	0.65
rG[b]	–0.65	–1.41	–0.28	–2.09
2′-O-MeG	–0.89	–1.79	–0.36	–0.86
2′-S-MeG	2.55	1.41	3.16	2.43

[a]Computed at HF/6–31G* optimized geometries.
Energies are in kcal/mol relative to the C2′-endo conformation.

Table 1 also includes the relative energies of 2′-O-methylguanosine and 2′-S-methylguanosine in C2′-endo and C3′-endo conformation. These data indicate that the electronic nature of C2′-substitution has a significant impact on the relative stability of these conformations. Substitution of the 2′-O-methyl group increases the preference for the C3′-endo conformation (when compared to riboguanosine) by ~0.4 kcal/mol at both the HF/6–31G* and MP2/6–31G*//HF/6–31G* levels. In contrast, the 2′-S-methyl group reverses the trend. The C2′-endo conformation is favored by ~2.6 kcal/mol at the HF/6–31G* level, while the same difference is reduced to 1.41 kcal/mol at the MP2/6–31G*//HF/6–31G* level. For comparison, and also to evaluate the accuracy of the molecular mechanical force-field parameters used for the 2′-O-methyl and 2′-S-methyl substituted nucleosides, we have calculated the gas phase energies of the nucleosides using the SPASMS module (33) of the AMBER4.1 package. The results reported in Table 1 indicate that the SPASMS calculated relative energies of these nucleosides compare qualitatively well with the *ab initio* calculations.

Additional calculations were also performed to gauge the effect of solvation on the relative stability of nucleoside conformations. The effect of aqueous solvation estimated by the SCI-PCM (self-consistent isodensity polarized continuum model) method (34) using HF/6–31G* geometries confirms that the relative energetic preference of the four nucleosides in the gas-phase is maintained in the aqueous phase as well (Table 1). Solvation effects were also examined using molecular dynamics simulations of the nucleosides in explicit water. The dynamic changes in sugar pucker of these four nucleosides are schematically represented in Figure 1a–d. From these trajectories, one can observe the predominance of C2′-endo conformation for deoxyriboguanosine and 2′-S-methylriboguanosine while the riboguanosine and 2′-O-methylriboguanosine prefer the C3′-endo conformation. These results are in much accord with the available NMR results on 2′-S-methylribonucleosides. NMR studies of sugar puckering equilibrium using vicinal spin-coupling constants have indicated that the conformation of the sugar ring in 2′-S-methylpyrimidine nucleosides show an average of >75% S-character, whereas the corresponding purine analogs exhibit an average of >90% S-pucker (22). It was also observed that the 2′-S-methyl substitution in deoxynucleoside confers more conformational rigidity to the sugar conformation when compared with deoxyribonucleosides (that are typically 65% S-pucker). This behavior is also reflected in Figure 1.

Structural features of DNA:RNA, OMe_DNA:RNA and SMe_DNA:RNA hybrids

The average RMS deviation of the DNA:RNA structure from the starting hybrid coordinates is shown in Figure 2a. The results

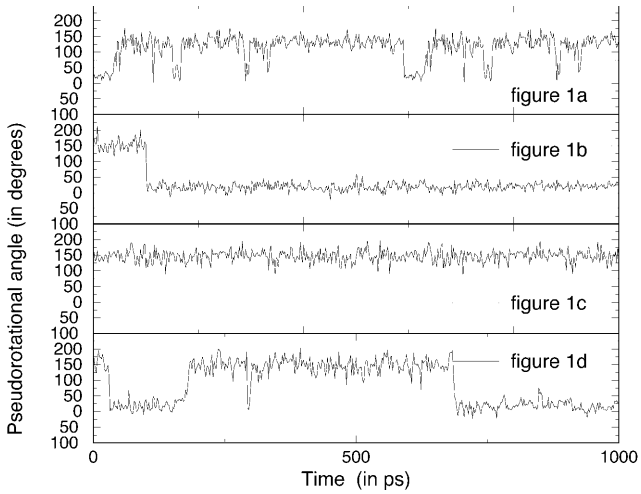

Figure 1. The time dependent changes in pseudorotational profiles of sugar ring conformation of (**a**) deoxyguanosine, (**b**) riboguanosine, (**c**) 2′-S-methyl and (**d**) 2′-O-methylguanosines.

indicate the structure is stabilized over the length of the simulation with an approximate average r.m.s. deviation of 1.0 Å. This deviation is due, in part, to inherent differences in averaged structures (i.e. the starting conformation) and structures at thermal equilibrium. The changes in sugar pucker conformation for three of the central base pairs of this hybrid are presented in Figure 3. These profiles are in good agreement with the observations made in previous NMR studies (35–37) as well as those reported by Cheatham and Kollman (24). From Figure 3, it is evident that the sugars in the RNA strand maintain very stable geometries in the C3′-endo conformation with ring pucker values near 0°. In contrast, the sugars of the DNA strand show significant variability. This is consistent with the work of Gonzalez *et al*. in which time average restraints were applied to examine the dynamic nature of sugar puckering in DNA:RNA hybrids (37). As in their study, the results indicate the DNA sugars are in dynamic equilibrium between the S and N domains, with an average conformation near the O4′-endo or E domain. It is important to point out, however, that the results presented here indicate the O4′-endo conformation is also populated, suggesting that this geometry contributes to the average structure as well.

The plots of the RMS deviations for OMe_DNA:RNA and SMe_DNA:RNA hybrids are shown in Figure 2b and c. The average RMS deviation of the OMe_DNA:RNA is ~1.2 Å from the starting A-form conformation while the SMe_DNA:RNA shows a slightly higher deviation (~1.8 Å) from the starting hybrid conformation. The SMe_DNA strand also shows a greater variance in RMS deviation, suggesting the S-methyl group may induce some structural fluctuations. The changes in sugar conformation for three of the central base pairs of the OMe_DNA:RNA and SMe_DNA:RNA hybrids are shown in Figure 3. Once again, the sugar puckers of the RNA complements maintain C3′-endo puckering throughout the simulation. As expected from the nucleoside calculations, however, significant differences are noted in the puckering of the OMe_DNA and SMe_DNA strands, with the former adopting C3′-endo, and the latter, C1′-exo/C2′-endo conformations. Although some variation in puckering is noted in the end groups due to base fraying effects

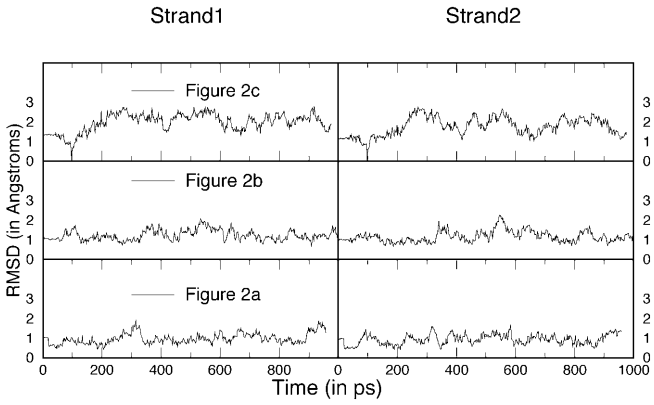

Figure 2. Plots of average RMS deviations of (**a**) SMe_DNA:RNA, (**b**) OMe_DNA:RNA and (**c**) DNA:RNA hybrids over the simulation time in comparison with corresponding starting conformations.

(not pictured), the sugar puckers of both AO strands are well stabilized throughout the simulation time. This is a sharp contrast to the dynamic behavior of the DNA sugars (discussed above), indicating the 2′-substitutions effectively 'lock' the sugar conformation in the AO strand.

An analysis of the helicoidal parameters for all three hybrid structures has also been performed to further characterize the duplex conformation. Three of the more important axis-base pair parameters that distinguish the different forms of the duplexes, X-displacement, propeller twist, and inclination, are reported in Table 2. Usually, an X-displacement near zero represents a B-form duplex while a negative displacement, which is a direct measure of deviation of the helix from the helical axis, makes the structure appear more A-like in conformation. In A-form duplexes, these values typically vary from –4 to –5 Å. In comparing these values for all three hybrids, the SMe_DNA:RNA hybrid shows the most deviation from the A-form value, the OMe_DNA:RNA shows the least, and the DNA:RNA is intermediate. A similar trend is also evident when comparing the inclination and propeller twist values with ideal A-form parameters. These results are further supported by an analysis of the backbone and glycosidic torsion angles of the hybrid structures. Glycosidic angles (χ) of A-form geometries, for example, are typically near –159° while B-form values are near –102°. These angles are found to be –162, –133 and –108° for the OMe_DNA, DNA and SMe_DNA strands, respectively. All RNA complements adopt a χ angle close to –160°. In addition, 'crankshaft' transitions were also noted in the backbone torsions of the central UpU steps of the RNA strand in the SMe_DNA:RNA and DNA:RNA hybrids. Such transitions have been noted in previous studies and suggest some local conformational changes may occur to relieve a less favorable global conformation (24,38). Taken overall, the results indicate the amount

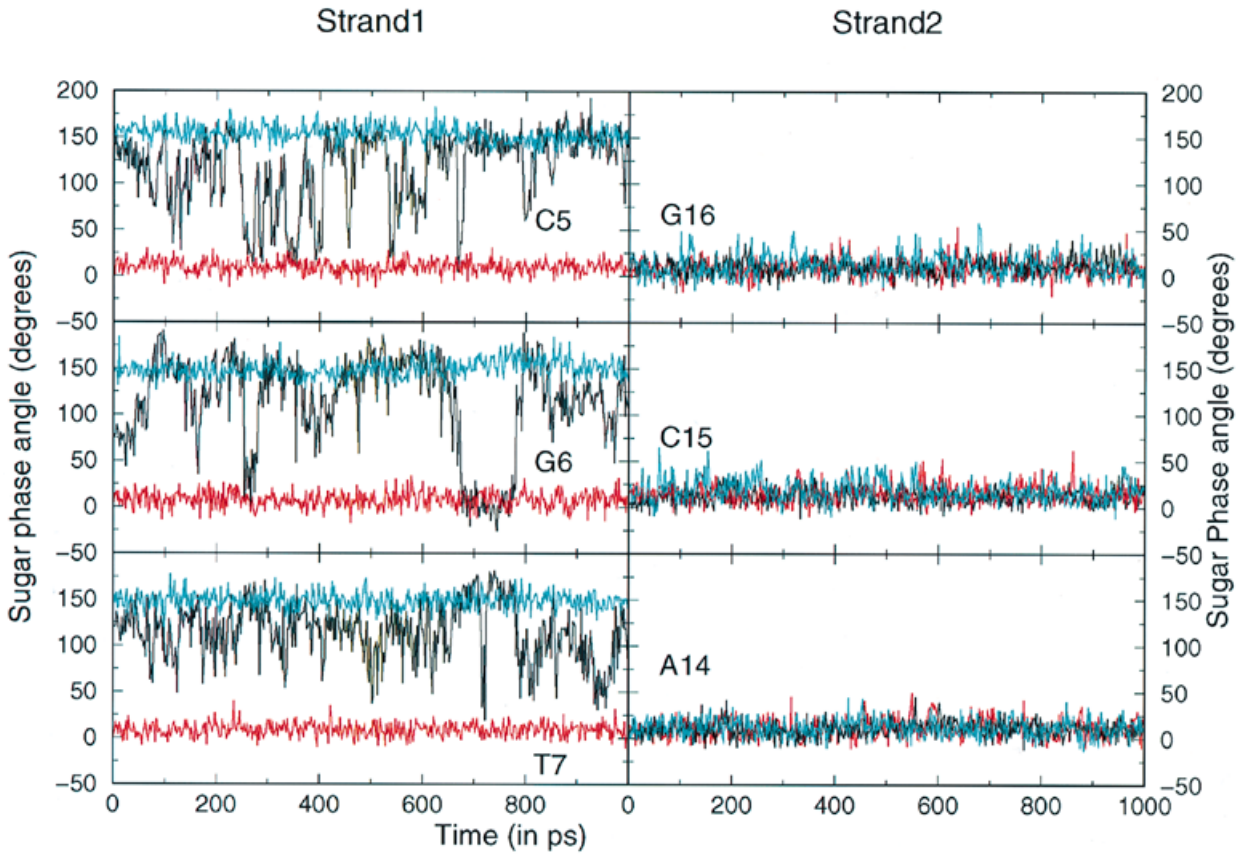

Figure 3. Sugar pucker pseudorotation changes over time for three of the central base pairs of the DNA:RNA (black), OMe_DNA:RNA (red) and SMe_DNA:RNA (blue) hybrids.

of A-character decreases as OMe_DNA:RNA>DNA:RNA> SMe_DNA:RNA, with the latter two adopting more intermediate conformations when compared to A- and B-form geometries. (A complete listing of the helical and backbone torsional parameters is given in the Supplementary Material.)

Stability of C2′-modified DNA:RNA hybrids

Although the overall stability of the DNA:RNA hybrids depends on several factors including sequence-dependencies and the purine content in the DNA or RNA strands, usually DNA:RNA hybrids are less stable than RNA:RNA duplexes, and in some cases even less stable than DNA:DNA duplexes (39,40). Available experimental data attributes the relatively lowered stability of DNA:RNA hybrids largely to its intermediate conformational nature between DNA:DNA (B-family) and RNA:RNA (A-family) duplexes (41–43). The overall thermodynamic stability of nucleic acid duplexes may originate from several factors including the conformation of backbone, base-pairing and stacking interactions. While it is difficult to ascertain the individual thermodynamic contributions to the overall stabilization of duplex, it is reasonable to argue that the major factors that promote increased stability of hybrid duplexes are due to better stacking interactions (electrostatic π–π interactions) and more favorable groove dimensions for hydration (44). Recent experimental studies indicate that OMe_DNA:RNA hybrids possess enhanced thermodynamic stability when compared to the RNA:RNA and DNA:RNA hybrids (45,46). However, the C2′-S-methyl substitution has been shown to destabilize the AO:RNA hybrid (unpublished results, ISIS Pharmaceuticals). The notable differences in the rise values among the three hybrids may offer some explanation. While the 2′-S-methyl group has a strong influence on decreasing the base-stacking through high rise values (~3.2 Å), the 2′-O-methyl group makes the overall structure more compact with a rise value that is equal to that of A-form duplexes (~2.6 Å). Despite its overall A-like structural features, the SMe_DNA:RNA hybrid structure possesses an average rise value of 3.2 Å which is quite close to that of B-family duplexes. In fact, some local base-steps (CG steps) may be observed to have unusually high rise values (as high as 4.5 Å). Thus, the greater destabilization of 2′-S-methyl substituted DNA:RNA hybrids may be partly attributed to poor stacking interactions.

Conformation and RNase H activity

While the main interest in developing modified oligonucleotides is to improve binding affinity towards complementary mRNA strands, another key element to antisense efficacy is RNase H recruitment and activity (47). In previous work, it has been postulated that RNase H binds to the minor groove of RNA:DNA hybrid complexes, requiring an intermediate minor groove width between ideal A- and B-form geometries to optimize interactions between the sugar phosphate backbone atoms and Asn16 and Asn45 of RNase H (48–50). A close inspection of the averaged structures for the three hybrids simulated reveals significant variation in the minor groove width dimensions as shown in Table 3. Whereas the O-methyl substitution leads to a slight expansion of the minor groove width when compared to the standard DNA:RNA complex, the S-methyl substitution leads to a general contraction (~0.9 Å). These changes are most likely due to the preferred sugar puckering noted for the antisense strands which induce either A- or B-like single strand conformations. In addition to minor groove variations, the results also point to potential differences in the steric makeup of the minor groove. As shown in Figure 4, the O-methyl group points into the minor groove while the S-methyl is directed away towards the major groove. Essentially, the S-methyl group has flipped through the bases into the major groove as a consequence of C2-endo puckering. Since recognition is postulated to occur in this region, it is reasonable to assume the O-methyl group may also play some role in deactivating the enzyme. Unfortunately, no RNase H data is yet available for C2′-S-methyl containing derivatives.

Table 2. Average helical parameters derived from the last 500 ps of simulation time

Helicoidal Parameter	B-DNA[a] (x-ray)	B-DNA[b] (fibre)	A-DNA (fibre)	DNA:RNA	OMe_DNA:RNA	SMe_DNA:RNA
X-disp	1.2	0.0	–5.3	–4.5	–5.4	–3.5
Inclination	–2.3	1.5	20.7	11.6	15.1	0.7
Propeller	–16.4	–13.3	–7.5	12.7	–15.8	–10.3

[a]ref. (51).
[b]Derived from model built structure using the NUCGEN program of AMBER.
Canonical A- and B-form values are given for comparison.

Table 3. Minor groove widths averaged over the last 500 ps of simulation time

Phosphate distance	DNA:RNA	OMe_DNA:RNA	SMe_DNA:RNA	DNA:DNA[a] (B-form)	RNA:RNA[a] (A-form)
P5–P20	15.27	16.82	13.73	14.19	17.32
P6–P19	15.52	16.79	15.73	12.66	17.12
P7–P18	15.19	16.40	14.08	11.10	16.60
P8–P17	15.07	16.12	14.00	10.98	16.14
P9–P16	15.29	16.25	14.98	11.65	16.93
P10–P15	15.37	16.57	13.92	14.05	17.69

[a]Distances taken from (24).

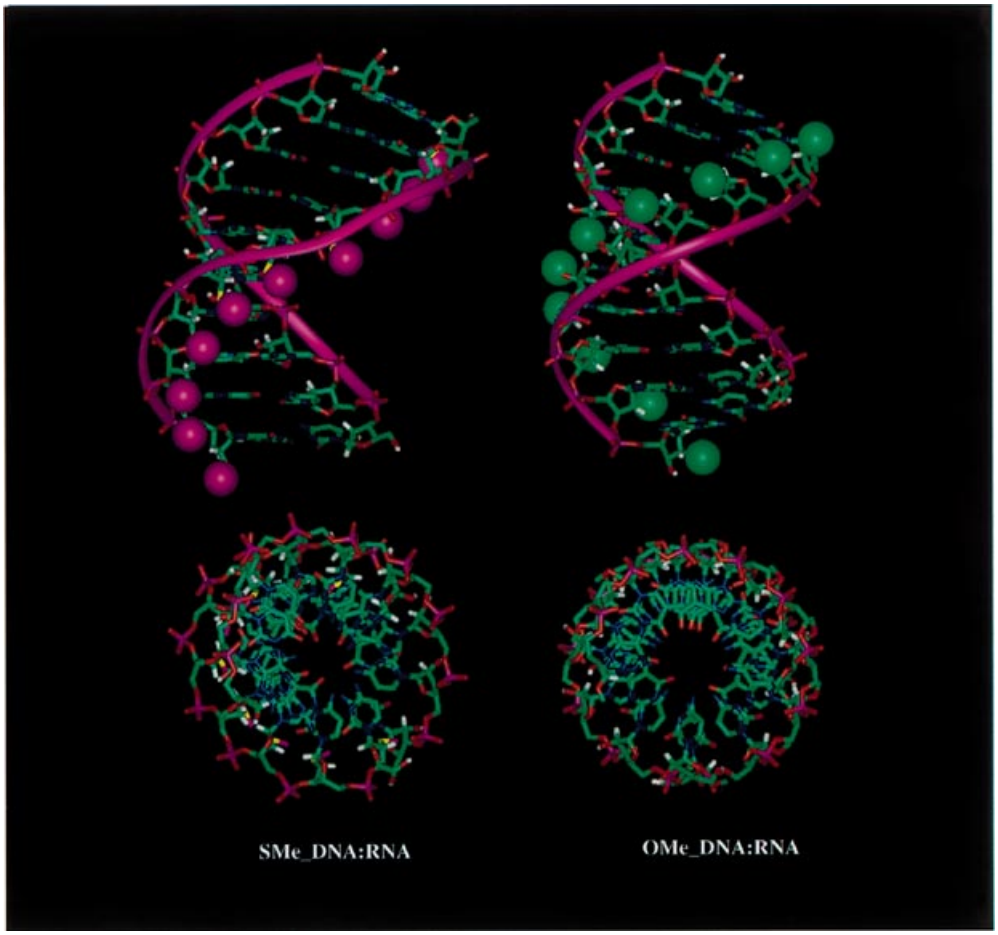

Figure 4. Orthogonal views of the SMe_DNA:RNA (left) and OMe_DNA:RNA complexes. The C2′-substitutions are highlighted with space-filling spheres.

CONCLUSIONS

This study has examined the structural properties of oligonucleotide complexes containing C2′-O-methyl and C2′-S-methyl groups using a combination of molecular dynamics, molecular mechanics and *ab initio* calculations. The primary goal of this work was to relate the conformational effects induced by these two stereochemically similar modifications with the observed differences in binding affinities as well as the potential impact these may have on RNase H recruitment and activation. Based on an analysis of sugar puckering and helicoidal parameters derived from MD simulations, the results show the OMe_DNA:RNA and SMe_DNA:RNA hybrids adopt unique structures as compared to native RNA:DNA complexes. Although all three hybrids loosely adhere to an A-form geometry, our results indicate A-form character diminishes according to the following trend: OMe_DNA:RNA>DNA:RNA>SMe_DNA:RNA. Interestingly, this trend also follows the known stability of these hybrids. Calculations of the free nucleosides indicate the preference for C3′-endo puckering also follows an analogous trend. Given the experimental melting temperatures for these hybrids (OMe_DNA:RNA>DNA:RNA>SMe_DNA:RNA), it is reasonable to conclude that antisense strand preorganization to favor A-form structures is, as hypothesized, one of the key elements to increasing binding affinities in complex formation. Obviously, sugar puckering is not the only factor effecting stability since some variability in melting temperature is noted across a wider series of C2′-O-X derivatives (3).

Although our study points to the preferred formation of C2-endo puckering as the primary effector in destabilizing C2′-S-methyl containing duplexes (due to inefficient base stacking and pairing), this may not fully explain the significant decrease in melting temperature noted as compared to native DNA:RNA hybrids. It is important to point out that both deoxyriboguanosine and 2′-S-methylguanosine favor C2′-endo puckering in the nucleoside. Although not reported in the body of this work, the MD trajectories did reveal considerable rotational flexibility in the C2′-SMe bond. While the C2′-OMe torsion is relatively fixed at gauche+, the C2′-S torsion populates both gauche+ and gauche– with equal probability. This may, in part, be due to the position of the S-methyl group that extends away from minor groove interactions. Alternatively, the C-S bond length may simply reduce the steric hindrance to methyl group rotation. Regardless of the origin, the flexibility is notable and suggests C2′-S-X derivatives may display other unique properties related to structure and stability.

Our study has also given an insight to the potential structural properties of AO:RNA hybrids that lead to RNase H recognition

and activation. While the OMe_DNA:RNA complex has a much wider minor groove width when compared with the natural DNA:RNA substrate, the SMe_DNA:RNA minor groove is narrower. The OMe_DNA:RNA hybrid adopts a conformation that is very close to the standard A-form geometry (of RNA:RNA complexes) which may explain the failure of this complex to effectively recruit RNase H activity. In addition, the results show the O-methyl group protrudes into the minor groove, which may play some role in sterically hindering recognition. The significance of this interaction could be further explored experimentally by testing the activity of OMe_DNA:DNA hybrids against RNase H. This potential substrate should adopt a fairly similar structure to the natural RNA:DNA substrate, allowing the steric effect of the O-methyl group to be scrutinized. In contrast to the OMe_DNA:RNA structure, the SMe_DNA:RNA hybrid appears to have structural parameters that more closely approximate those of the natural substrate. Although the minor groove is slightly narrower than that of the standard RNA:DNA hybrid, the S-methyl group occupies a position that points away from the minor groove. Since no RNase H binding data is available for the S-methyl derivative, it is not possible to determine if C2′-S-X substitutions harbor potential benefits to antisense drug development. Since it is becoming ever more apparent that C2′-O-X derivatives may lack the necessary structural qualities to effectively recruit RNase H, new information regarding alternative substitutions that are successful in this regard may provide new routes to the rational design of antisense drugs.

The Supplementary Material includes a listing of force field partial charges and atom types, tables of helical and backbone parameters, figures of backbone changes and structural coordinates in PDB format.

See supplementary material available in NAR Online.

REFERENCES

1 Cohen,J.S. (ed.) (1989) *Oligodeoxynucleotides: Antisense Inhibitors of Gene Expression*. CRC Press Inc., Boca Raton, FL, USA.
2 Crooke,S.T. (1996) In Teicher,B.A. (ed.), *Cancer Therapeutics: Experimental and Clinical Agents.* Humana Press, Totowa, NJ, pp. 229–335.
3 Freier,S.M. and Altmann,K.-H. (1997) *Nucleic Acids Res*., **25**, 4429–4443.
4 Goodchild,J. (1990*) Bioconjug. Chem*., **1**, 165–187.
5 Uhlmann,E. and Peyman,A. (1990) *Chem. Rev*., **90**, 543–584.
6 De Mesmaeker,R.A., Altman,K.-H., Waldner,A. and Wendeborns,S. (1995) *Curr. Opin. Struct. Biol*., **5**, 343–355.
7 Wagner,R.W., Matteucci,M.D., Lewis,J.G., Gutierrez,A.J., Moulds,C. and Froehler,B.C. (1992) *Science*, **260**, 1510–1513.
8 Mesmaeker,A.E., Haner,R., Martin,P. and Moser,H.E. (1995) *Acc. Chem. Res*., **28**, 366–374.
9 Koziolkiewicz,M., Krakowiak,A., Kwinkowski,M., Boczkowska,M. and Stec,W.J. (1995) *Nucleic Acids Res*., **23**, 5000–5005.
10 Bachelin,M., Hessler,G., Kurz,G., Hacia,J.G., Dervan,P.B. and Kessler,H. (1998*) Nature Struct. Biol*., **5**, 271–276.
11 Saenger,W. (1984) *Principles of Nucleic Acid Structure*. Springer-Verlag, New York, NY.
12 Guschlbauer,W. and Jankowski,K. (1980) *Nucleic Acids Res*., **8**, 1421–1433.
13 Sanghvi,Y.S. and Cook,P.D. (eds) (1994*) Carbohydrate Modifications in Antisense Research, ACS Symposium Series No. 580.* American Chemical Society, Washington, DC.
14 Morvan,F., Porumb,H., Degols,G., Lefebre,I., Pompon,A., Sproat,B.S., Malvy,C., Lebleu,B.and Imbach,J.-M. (1993) *J. Med. Chem*., **36**, 280–287.
15 Kawasaki,A.M., Casper,M.D., Freier,S.M., Lesnik,E.A., Zounes,M.C., Cummins,L.L., Gonzalez,C. and Cook,P.D. (1993) *J. Med. Chem*., **36**, 831–841.
16 Crooke,S.T, Lemonidis,K.M, Neilson,L., Griffey,R., Lesnik,E.A. and Monia,B.P. (1995) *Biochem. J*., **312**, 599–608.
17 Dash,P., Lotan,I., Knapp,M., Kandell,E.R. and Goelet,P. (1987*) Proc. Natl Acad. Sci. USA*, **22**, 7896–7900.
18 Fedoroff,O.Y., Salazar,M. and Reid,B.R. (1993) *J. Mol. Biol*., **233**, 509–523.
19 Nakamura,H., Oda,Y., Iwai,S., Inoue,H., Ohtsuka,E., Kanaya,S., Kimura,S., Katsuda,C., Katayanagi,K., Morikawa,K., Miyashiro,H. and Ikehara,M. (1991) *Biochemistry*, **88**, 11535–11539.
20 Inoue,H., Hayase,Y., Iwai,S. and Ohtsuka,E. (1987) *FEBS Lett*., **215**, 327–330.
21 Schmit,C., Bèvierre,M.-O., De Mesmaeker,A. and Altmann,K.-H. (1994) *Bioorg. Med. Chem. Lett*., **4**, 1969–1974.
22 Fraser,A., Wheeler,P., Cook,P.D. and Sanghvi,Y.S. (1993) *J. Heterocycl. Chem*., **30**, 1277–1287.
23 Aurup,H., Tuschl,T., Benseler,F., Ludwig,J. and Eckstein,F. (1994) *Nucleic Acids Res*., **22**, 20–24.
24 Cheatham,T.E. and Kollman,P.A. (1997) *J. Am. Chem. Soc*., **119**, 4805–4825.
25 Pearlman,D.A., Case,D.A., Caldwell,J.W., Ross,W.R., Cheatham,T.E.,III, Ferguson,D.M., Seibel,G.L., Singh,U.C., Weiner,P.K. and Kollman,P.A. (1995) *AMBER 4.1*. University of California, San Francisco, CA.
26 Jorgensen,W.L., Chandrasekhar,J. and Madhura,J.D. (1983) *J. Comput. Chem*., **14**, 89.
27 Essman,U., Perera,L., Berkowitz,M.L., Darden,T., Lee,H. and Pedersen,L.G. (1995) *J. Chem. Phys*., **103**, 8577–8593.
28 Ryckaert,J.P., Ciccotti,G. and Berendsen,H.J.C. (1977) *J. Comp. Phys*., **23**, 327–341.
29 Lavery,R and Sklenar,H. (1995) *Curves 5.1*. Institut de Biologie Physico-Chimique, Paris, France.
30 Bayly,C., Cieplak,P., Cornell,W. and Kollman,P.A. (1993) *J. Phys. Chem*., **97**, 10269–10280.
31 Cornell,W.D., Cieplak,P., Bayly,C.I., Gould,I.R., Merz,K.M., Ferguson,D.M., Spellmeyer,D.C., Fox,T., Caldwell,J.W. and Kollman,P.A. (1995) *J. Am. Chem. Soc*., **117**, 5179–5197.
32 Frisch,M.J., Trucks,G.W., Schlegel,H.B., Gill,P.M.W., Johnson,B.G., Robb,M.A., Cheeseman,J.R., Keith,T., Petersson,G.A., Montgomery,J.A., Raghavachari,K., Al-Laham,M.A., Zakrzewski,V.G., Ortiz,J.V., Foresman,J.B., Cioslowski,J., Stefanov,B.B., Nanayakkara,A., Challacombe,M., Peng,C.Y., Ayala,P.Y., Chen,W., Wong,M.W., Andres,J.L., Replogle,E.S., Gomperts,R., Martin,R.L., Fox,D.J., Binkley,J.S., Defrees,D.J., Baker,J., Stewart,J.P., Head-Gordon,M., Gonzalez,C. and Pople,J.A., (1995) *Gaussian 94*, Revision E.2, Gaussian, Inc., Pittsburgh, PA.
33 Spellmeyer,D.C., Swope,W.C., Evensen,E.-R., Ferguson,D.M. (1994) *SPASMS*. University of California, San Francisco, CA.
34 Wong,M.W., Wiberg,K.B. and Frisch,M.J. (1996) *J. Comp. Chem*., **16**, 385.
35 Chou,S.-H., Flynn,P. and Reid,B. (1989) *Biochemistry*, **28**, 2435–2443.
36 Salazar,M., Fedoroff,O.Y., Miller,J.M., Riberiro,S.N. and Reid,B.R. (1993) *Biochemistry*, **32**, 4207–4215.
37 Gonzalez,C., Stec,W., Reynolds,M.A. and James,T.L. (1995) *Biochemistry*, **34**, 4969–4982.
38 Weisz,K., Shafer,R.H., Egan,W. and James,T.L. (1994) *Biochemistry*, **33**, 354–366.
39 Hall,K.B. and McLaughlin,L.W. (1991) *Biochemistry*, **30**, 10606–10613.
40 Roberts,W.R. and Crothers,D.M. (1992) *Science*, **258**, 1463–1466.
41 Gyi,J.I., Conn,G.L., Lane,A.N. and Brown,T. (1996) *Biochemistry*, **35**, 12538–12548.
42 Gyi,J.I., Conn,G.L., Lane,A.N. and Brown,T. (1998) *Biochemistry*, **37**, 73–80.
43 Lesnik,E.A. and Freier,S.M. (1995) *Biochemistry*, **34**, 10807–10815.
44 SantaLucia,J., Kierzek,R. and Turner,D.H. (1992) *Science*, **256**, 217–219.
45 Lesnik,E.A. and Freier,S.M. (1998) *Biochemistry*, **37**, 6991–6997.
46 Crooke,S.T., Lemonidis,K.M., Neilson,L., Girffey,R., Lesnik,E.A. and Monia,B.P. (1995) *Biochem. J*., **312**, 599–608.
47 Tidd,D.M. (1994) *Antisense Res. Dev*., **5**, 23.
48 Searle,M.S. and Williams,D.H. (1993) *Nucleic Acids Res*., **21**, 2051–2056.
49 Milligan,J.F., Matteucci,M.D. and Martin,J.C. (1993) *J. Med. Chem*., **36**, 1923–1937.
50 Furdon,P.J., Dominski,Z. and Kole,R. (1989) *Nucleic Acids Res*., **17**, 9193–9204.
51 Prive,G.G., Yanagi,K. and Dickerson,R.E. (1991) *J. Mol. Biol*., **217**, 177–199.